Proc. Natl. Acad. Sci. USA
Vol. 89, pp. 11664–11668, December 1992
Neurobiology

Suppression of the onset of myelination extends the permissive period for the functional repair of embryonic spinal cord

(chicken/spinal cord injury/oligodendrocyte/dysmyelination)

HANS S. KEIRSTEAD, SOHAIL J. HASAN, GILLIAN D. MUIR, AND JOHN D. STEEVES*

Departments of Zoology and Anatomy, University of British Columbia, Vancouver, BC, V6T 1Z4, Canada

Communicated by Victor Hamburger, August 14, 1992

ABSTRACT **In an embryonic chicken, transection of the thoracic spinal cord prior to embryonic day (E) 13 (of the 21-day developmental period) results in complete neuroanatomical repair and functional locomotor recovery. Conversely, repair rapidly diminishes following a transection on E13–E14 and is nonexistent after an E15 transection. The myelination of fiber tracts within the spinal cord also begins on E13, coincident with the transition from permissive to restrictive repair periods. The onset of myelination can be delayed (dysmyelination) until later in development by the direct injection into the thoracic cord on E9–E12 of a monoclonal antibody to galactocerebroside, plus homologous complement. In such a dysmyelinated embryo, a subsequent transection of the thoracic cord as late as E15 resulted in complete neuroanatomical repair and functional recovery (i.e., extended the permissive period for repair).**

Although vertebrate central nervous system (CNS) axons will not regrow in the environment of the adult spinal cord (1, 2), peripheral nerve grafts into the CNS provide a favorable environment through which CNS axons will regenerate (3–5). These findings indicate that adult brainstem–spinal neurons retain intrinsic axonal growth programs and, if given (as yet unknown) favorable CNS environmental conditions, should be capable of successfully regenerating axons. Since the CNS extraneuronal environment of the developing embryo favors axonal outgrowth, comparing and contrasting the development and repair of embryonic brainstem–spinal projections should elucidate mechanisms essential to the functional repair of injured adult spinal cord.

The anatomical development and functional organization of avian descending brainstem–spinal pathways concerned with locomotion is similar to that of other vertebrates, including mammals (1, 5–10). If the thoracic spinal cord of an embryonic chicken is transected prior to day 13 (E13) of the 21-day developmental period, the animal will subsequently effect complete neuroanatomical and physiological repair resulting in total functional recovery (8–10). Most importantly, regeneration of previously severed axonal fibers contributes to this repair process (10). We have termed the developmental period prior to E13 the *permissive period* for functional repair. If the spinal cord is transected on or after E13, the repair of descending supraspinal pathways rapidly diminishes, resulting in minimal or no functional recovery (8–10). Transection on or after E15 results in no axonal repair or functional recovery (1, 2, 8–10). For these reasons we have termed the developmental period on or after E13 the *restrictive period* for functional repair.

Myelin-associated proteins that inhibit the anatomical growth of axons *in vitro* (11) as well as the regrowth of axotomized corticospinal fibers *in vivo* (12) have been identified in rat spinal cord. Thus, it is noteworthy that the onset of myelination in the developing chicken spinal cord starts around E13 (13–15), coincident with the transition from the permissive period to the restrictive period for repair. To assess a potential inhibitory role for myelin in the functional regeneration of brainstem–spinal projections after spinal transection in the embryonic chicken, we delayed the onset of myelination (dysmyelination) until well into the restrictive period for embryonic spinal cord repair.

MATERIALS AND METHODS

Fertilized White Leghorn eggs were incubated at 37°C in an automatic rotating incubator. Control and experimental eggs were staged by using the accepted protocol of Hamburger and Hamilton (16). After every surgical procedure, each egg was sealed and returned to the incubator.

Dysmyelination. To cause dysmyelination, the thoracic spinal cord was pressure injected at E9–E12 by using a glass micropipette (tip diameter, 30–40 μm) connected to a Picospritzer II pump (General Valve Corp., Fairfield, NJ). Injections consisted of an IgG3 mouse galactocerebroside (GalC) antibody (a gift from B. Ranscht, La Jolla Cancer Research Foundation, La Jolla, CA) plus 20% homologous serum (as a source of complement) in 0.1 M phosphate-buffered saline (PBS, pH 7.4). Each animal received a total volume of 2–3 μl, over one to four penetrations, injected directly into the mid-to-high thoracic spinal cord. The GalC antibody was supplied as a hybridoma supernatant (2.67 mg/ml), which was then diluted 1:25, providing an effective concentration of 63.0 ng of GalC hybridoma supernatant injected per gram of body weight.

To control for nonspecific binding of the GalC antibody, control embryos were similarly injected with 20% homologous serum complement plus a human antibody that does not crossreact with chicken. We chose a monoclonal antibody to glial fibrillary acidic protein (GFAP), a major constituent of astrocytes within the CNS. Other immunological control embryos received injections of (*i*) the GalC antibody only, (*ii*) homologous serum complement proteins only, (*iii*) vehicle only (0.1 M PBS, pH 7.4), or (*iv*) the GalC antibody plus homologous serum, following heat inactivation of the complement by exposure at 50°C for 30 min.

Those embryos not undergoing a subsequent thoracic spinal cord transection were perfused intracardially at the appropriate developmental stage (see *Results*) with 0.1 M PBS containing 2500 USP units of heparin in 50 ml of PBS, pH 7.4 (37°C), followed by perfusion with 4% paraformaldehyde in 0.1 M phosphate buffer, pH 7.4 (4°C). The dissected

The publication costs of this article were defrayed in part by page charge payment. This article must therefore be hereby marked "*advertisement*" in accordance with 18 U.S.C. §1734 solely to indicate this fact.

Abbreviations: CNS, central nervous system; EMG, electromyographic; GalC, galactocerebroside; GFAP, glial fibrillary acidic protein; MBP, myelin basic protein; RDA, tetramethylrhodamine-labeled dextran amine; E*n*, embryonic day *n*; P*n*, post-hatching day *n*.

*To whom reprint requests should be addressed.

brains and/or spinal cords were subsequently embedded in paraffin by standard protocols.

Immunocytochemical Assessments. Parasagittal 10-μm sections were mounted on gelatin-coated slides and tested for myelin basic protein (MBP) immunoreactivity by standard indirect immunofluorescence techniques. The primary antibody was a rabbit anti-human MBP (Accurate Chemical Scientific Corp., Westbury, NY; #AXL746) and the secondary antibody was a fluorescein-conjugated goat anti-rabbit immunoglobulin (Caltag, South San Francisco; #L42001); both were diluted 1:100. Photomicrographs were taken on a Zeiss Axiophot using epifluorescent illumination.

Transection. Transections on E15 consisted of a pinch lesion of the high- to mid-thoracic spinal cord, applied with sharpened Dumont no. 5-45 forceps. To ensure that the spinal cord was completely severed, a no. 00 pin (marked to the appropriate depth of the cord for that stage of development) was then passed through the lesion, across the entire width of cord (for details, see ref. 9).

Neuroanatomical Assessments of Brainstem–Spinal Projections. On post-hatching day (P) 2, birds were anesthetized with an intramuscular injection of ketamine hydrochloride (30 mg/kg of body weight) plus xylazine hydrochloride (3 mg/kg). After removal of the dorsal vertebrae overlying the rostral lumbar cord, 0.2–1.0 μl of 25% tetramethylrhodamine-labeled dextran amine (RDA) (Molecular Probes, M_r 10,000, catalogue no. D-1817) in 2.5% (vol/vol) Triton X-100 diluted in 0.1 M Tris buffer (pH 9.0) was directly injected into the spinal cord by using a glass micropipette (tip diameter, 40–50 μm) attached to a Picospritzer II pump. Previous studies in our lab have indicated that this amount of RDA, injected at this level of the cord, remains confined to the lumbar level (i.e., does not diffuse rostrally to or above the site of transection) and within 24–48 hr is retrogradely transported via brainstem–spinal axons to the cell bodies of origin, with no trans-synaptic transport to brainstem neurons not having spinal projections (9, 10). After 48 hr, the P4 birds were given a lethal intramuscular injection of anesthetic (sodium pentobarbital, 75 mg/kg) and then perfused and fixed as outlined above. Each brainstem was sectioned (40 μm) in the transverse plane with a liquid-CO_2 freezing microtome. The number and position of retrogradely labeled brainstem–spinal neurons were then plotted and photographed under a microscope.

Functional Assessments. Intramuscular bipolar electromyographic (EMG) electrodes (0.003-in. diameter Teflon-coated stainless steel wire) were implanted percutaneously in four identified leg muscles (see *Results*) of each P3 hatchling chick under 1% halothane anesthesia on a background of 95% O_2/5% CO_2. After complete recovery from anesthesia (≈8 hr), EMG leg activity was recorded as each chick walked over ground along a straight path. EMG signals were amplified, bandpass filtered, and analyzed on a computer.

RESULTS

Ontogeny of Myelination. In 30 normally developing embryos, MBP immunoreactivity was not detected throughout the entire embryonic spinal cord prior to E13 (Fig. 1*A*). Myelination was first noticed within the ventrolateral funiculi of the cervical spinal cord on E13. Myelination appeared to proceed in a rostral–caudal direction. By E14, all levels of the spinal cord displayed at least some MBP immunoreactivity. On E15, a dense network of MBP immunoreactivity was observed within the spinal cord white matter of all 20 embryos examined (Fig. 1*B*). A second wave of myelination at E17 was suggested by a sudden increase in the density of MBP immunoreactivity at this stage of development (results not shown). A qualitative assessment of MBP immunofluorescence indicated that spinal cord myelination was completed by the time of hatching.

Dysmyelination. The delay in the onset of myelination (dysmyelination) of the spinal cord was initiated on E9–E12 by pressure injection of GalC antibody plus complement directly into the thoracic spinal cord. Immunocytochemical analysis of dysmyelinated spinal cord tissue 4–7 days later, on E13–E16, showed a complete lack of MBP immunoreactivity throughout the spinal cord (Fig. 1*C*) except for the most rostral one to four (cervical) segments of the cord. None of the 18 dysmyelinated embryos examined at E15 showed significant differences in the degree or extent of the suppression of spinal cord myelination. The onset of myelination was delayed for at least 4 days and was consistently found to occur on E17 (n = 9).

To control for the possible influence of nonspecific binding of the GalC antibody by other cell types, the thoracic spinal cords of 5 control embryos at E9–E12 were injected with an antibody to GFAP plus homologous complement. Myelination was not suppressed, nor was there any evidence of neuroanatomical repair or functional recovery after an E15 spinal transection in these animals or any other immunological control embryos. Other immunological control embryos received injections of GalC antibody only (n = 6), homologous serum complement proteins only (n = 8), PBS vehicle only (n = 4), or GalC antibody plus heat-inactivated serum (n = 8). In all cases, there was no delay in spinal cord myelination (see Fig. 1*D*). This indicates that both the GalC antibody and homologous serum complement proteins are necessary to suppress the onset of myelination.

Dysmyelination and Transection. Neuroanatomical or functional assessments were conducted on (*i*) 18 dysmyelinated E15 transected embryos, (*ii*) 8 normally myelinated (i.e., uninjected) E15 transected control animals, (*iii*) 6 immunological control E15 transected animals (see above), and (*iv*) 8 normally myelinated and untransected control animals. Neuroanatomical and functional assessments were often carried out on the same animal.

To ensure that the thoracic spinal cord was completely severed, randomly selected embryos were processed for histological examination immediately after the transection procedure. In all cases a complete transection was confirmed (see ref. 9). In addition, the lumbar spinal cords of 3 dysmyelinated embryos were injected with 1.0 μl of RDA solution (see below) at the time of the thoracic spinal cord transection. Only a complete thoracic transection would prevent the retrograde transport of any neuroanatomical tracer injected in this manner. Subsequent examination of the brainstem and spinal cord, rostral to the transection site, showed no evidence of RDA neuronal or axonal labeling; however, axonal labeling was evident near the injection site within the lumbar spinal cord. This confirms that the transection procedure reliably severs the entire thoracic spinal cord.

Neuroanatomical Assessments. There was a similar distribution and number of retrogradely labeled reticulospinal neurons in the 18 dysmyelinated, E15-transected experimental animals and 8 normally myelinated, untransected control animals following a post-hatching injection of RDA into the lumbar cord (Fig. 2). In contrast, the 8 normally myelinated and 6 immunological control embryos transected on E15 showed no retrogradely labeled brainstem–spinal neurons.

Within the ventromedial reticular formation of the pons, the dysmyelinated, E15-transected experimental animals averaged 1003 retrogradely labeled reticulospinal neurons per animal (range, 920–1292 cells); likewise the normally myelinated, untransected control animals averaged 1043 retrogradely labeled reticulospinal neurons per animal (range, 692–1311 cells). Comparable numbers and distributions of retrogradely labeled neurons were also noted for other brainstem–spinal projections from the vestibular nucleus, red

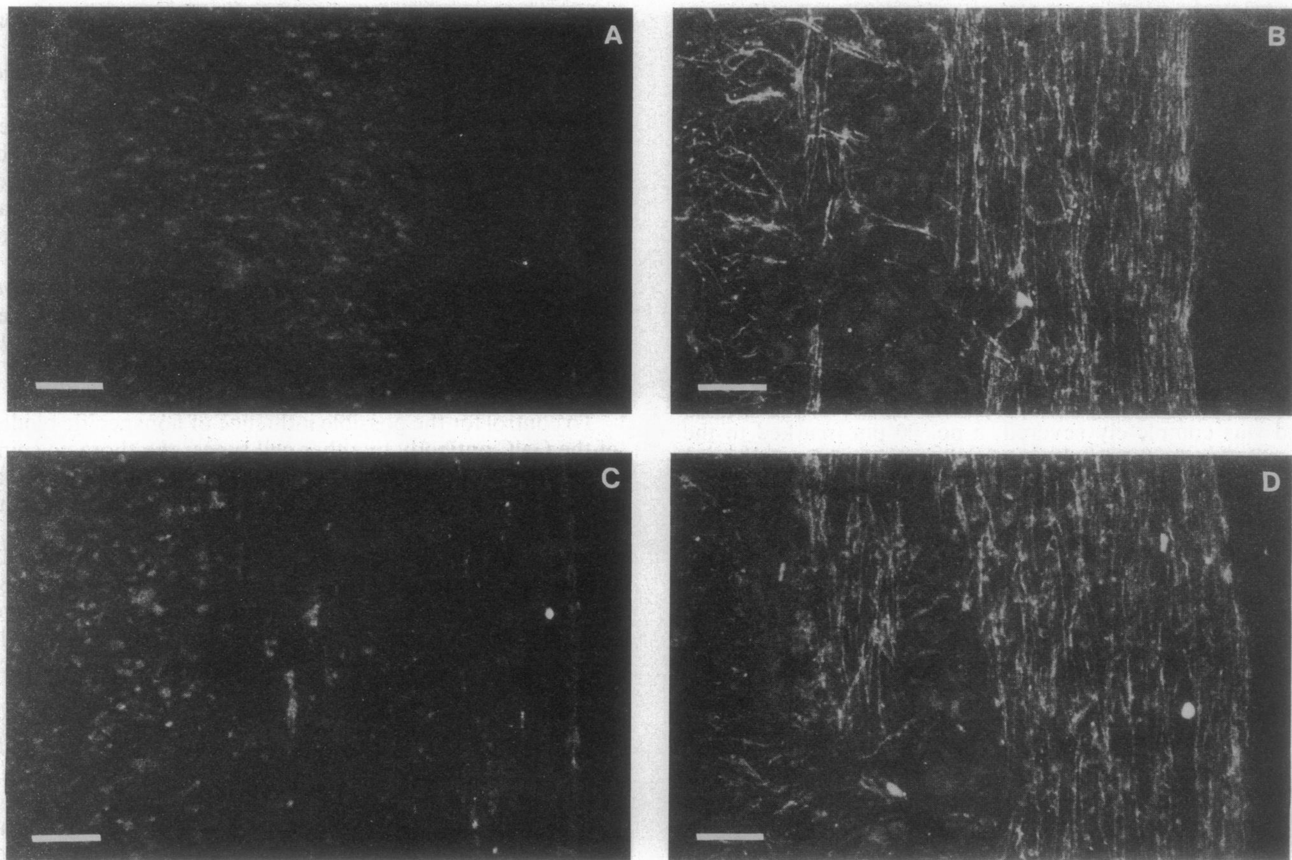

FIG. 1. MBP immunofluorescence staining of embryonic chicken spinal cord white matter in parasaggital section. (A) Unoperated control E12 thoracic spinal cord showing no MBP staining. (B) Unoperated normally myelinated (control) E15 thoracic spinal cord showing extensive MBP staining within white matter; MBP immunofluorescence first appears at E13. (C) E15 thoracic spinal cord from a dysmyelinated animal that received a single injection of GalC antibody plus homologous serum complement at E10; note the absence of myelination. (D) E15 thoracic spinal cord from an immunological control animal that received a single injection of serum complement only at E10; note that MBP staining of white matter is comparable to normally myelinated levels indicated in B. Normal myelination is also observed in the other immunological control animals. (Bars = 50 μm for A; 100 μm for B–D.)

nucleus, locus ceruleus, subceruleus nucleus, and raphe nucleus. These data indicate that neuroanatomical repair was not restricted to a few brainstem–spinal neurons (9, 10).

Further evidence for dysmyelination extending the permissive period for axonal repair was obtained from 3 dysmyelinated animals injected with RDA into the lumbar cord at the time of the E15 thoracic transection, and then a second retrograde fluorescent tracer (cascade blue-labeled dextran amine) on P4. We found no evidence of brainstem–spinal neurons retrogradely labeled with RDA, but there were many cascade blue-labeled neurons (results not shown) indicating the subsequent axonal repair/regeneration of descending projections after transection.

Functional Assessments. EMG recordings from leg muscles during post-hatching walking by a normally myelinated, untransected control chick and a dysmyelinated, E15-transected chick are shown in Fig. 3 A and B. The pattern of leg muscle activity obtained from dysmyelinated, E15-transected chicks did not differ from those obtained from normally myelinated, untransected control chicks. As expected during walking, the same muscle (e.g., lateral gastrocnemius muscle, an ankle extensor muscle) in the right and left leg showed alternating periods of activity (Fig. 3A). In addition, an antagonist muscle of the right lateral gastrocnemius, the sartorius (a knee extensor/hip flexor muscle) also exhibited activity that alternated with that of the right lateral gastrocnemius (Fig. 3A). The right iliofibularis (knee flexor/hip extensor) burst concurrently with the right lateral gastrocnemius and alternated with the right sartorius. None of the normally myelinated, E15-transected chicks were capable of locomotion or even unsupported standing.

The relationships between muscle activity (burst duration) and step cycle duration for normally myelinated, untransected control and dysmyelinated, E15-transected chicks were also similar (Fig. 3 C and D). The lateral gastrocnemius muscle is active during the weight-bearing phase (stance phase) of the step cycle. As cycle duration increases (i.e., the animal's velocity decreases), the duration of the stance phase increases, as does the burst duration of the lateral gastrocnemius muscle (17). Conversely, the sartorius muscle is active during the non-weight-bearing phase (swing phase) of the step cycle. As cycle duration increases, the duration of the swing phase remains relatively constant, as does the burst duration of the sartorius muscle (17). This supports the observation that the suppression of the onset of myelination extends the permissive period for functional spinal cord repair in the embryonic chicken. Normally myelinated control animals or immunological control animals, transected on E15, showed no functional recovery.

DISCUSSION

We have confirmed that the onset of myelination in the embryonic chicken spinal cord occurs at E13 (Fig. 1), which coincides with the transition from the permissive to restrictive period for the functional repair of injured spinal cord (8–10, 13–15). More importantly, we have delayed the onset of myelination (dysmyelination) until E17 by means of a

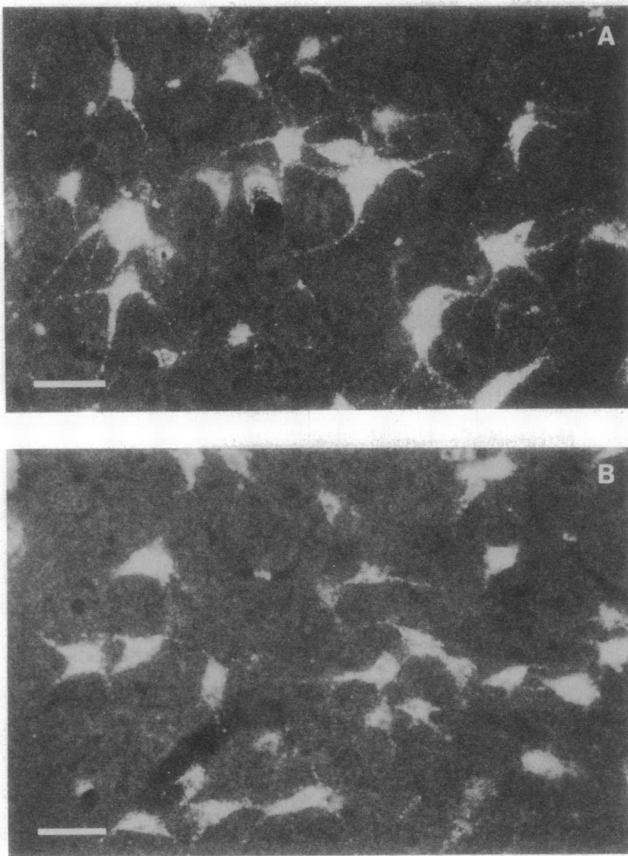

FIG. 2. Photomicrographs of retrogradely labeled gigantocellular reticulospinal neurons within the ventromedial reticular formation of the caudal pons in P4 chicks. Brainstem–spinal neurons were labeled by the retrograde axonal transport of RDA injected into the lumbar spinal cord on P2 and allowed 2 days for transport. (*A*) Normally myelinated, unoperated (control) hatchling. (*B*) Experimental hatchling that was subjected to embryonic dysmyelination on E10, followed by a complete transection of the thoracic spinal cord on E15. Note the similar number and distribution of retrogradely labeled reticulospinal neurons. Comparable anatomical repair was evident for other brainstem–spinal projections. (Bars = 50 μm.)

spinal injection of GalC antibody and serum complement, to determine whether myelin inhibits anatomical and functional repair following a transection. The immunological suppression of myelination until E17 was confirmed by MBP immunohistochemistry (Fig. 1) and either a modified thionine or Sudan black histological stain for myelin (results not shown). The dysmyelination procedure also suppresses the expression of several proteins that normally appear at the developmental onset of myelination in the chicken embryo (D. W. Ethell, H.S.K., J.D.S., unpublished work).

A thoracic spinal cord transection as late as E15 (i.e., during the normally restrictive period for repair) in dysmyelinated embryos resulted in complete neuroanatomical repair and functional recovery (Figs. 2 and 3). The number of retrogradely-labeled brainstem–spinal neurons and the quality of the voluntary locomotion observed in all dysmyelinated, E15-transected chicks were comparable to that in normally myelinated, control hatchling chicks that had not been transected. The neuroanatomical repair and functional recovery were also equivalent to that observed in chicks transected during the permissive period for spinal cord repair (e.g., E11–E12, when myelin has yet to appear; refs. 8–10). This is in sharp contrast to normally myelinated (control) embryos transected during the restrictive repair period (on E15), which, upon hatching, were completely paralyzed and unable to stand (regardless of whether they were previously injected with GalC antibody alone, complement alone, vehicle alone, PBS vehicle alone, GFAP antibody and complement, or GalC antibody and heat-inactivated serum).

It is arguable that the locomotor recovery observed in the dysmyelinated, E15-transected chicks was not dependent on the functional repair/regeneration of brainstem–spinal projections but was due to intrinsic activity of neural networks confined to the lumbar spinal cord (1, 2, 5). If this were the case, however, it is unlikely that the locomotor abilities would have been so equivalent (1). Further evidence comes from our previous demonstration in late embryos and hatchling chicks that direct focal stimulation of brainstem–spinal neurons, within the gigantocellular reticular formation (an identified brainstem locomotor region), elicited locomotor activity only in an animal transected prior to E13 (9, 10, 18). All the available evidence suggests that the high quality of functional locomotor recovery in dysmyelinated, E15-transected animals is due to the functional repair/regeneration of brainstem–spinal connections.

Antisera against GalC, the major oligodendrocyte sphingolipid (19), have been shown to demyelinate CNS tissue *in vitro* (20, 21) and optic nerve (22, 23) and spinal cord (24) *in vivo*. GalC is highly conserved across species and the GalC antibody used here exhibits specificity for chicken oligodendrocytes (19). Since chicken embryo CNS oligodendrocytes express GalC upon differentiation, 2–3 days prior to myelin formation (13), we injected the GalC antibody and serum complement on E9–E12. Although this protocol reliably evokes dysmyelination, it does not alter normal neuronal development as indicated by immunostaining for microtubule-associated protein 2 (ref. 25, MAP-2 for dendritic morphology), as well as thionin staining (results not shown).

We are uncertain whether the oligodendrocyte cell bodies survive our dysmyelination procedure. *In vitro*, the proposed mechanism of anti-GalC-induced demyelination involves microtubule disassembly and retraction of oligodendrocyte processes mediated by an influx of extracellular calcium (21). If chick oligodendrocyte cell bodies are preserved throughout dysmyelination *in vivo*, then the subsequent appearance of myelin may be due to the re-extension of processes from surviving oligodendrocyte cell bodies. If the oligodendrocyte cell bodies are destroyed by the dysmyelination procedure, then the subsequent myelination must be due to the novel differentiation of oligodendrocyte progenitors. These two possibilities are not mutually exclusive. The cellular site(s) for dysmyelination could be investigated by using double immunohistochemical staining with two different antibodies, one for the oligodendrocyte cell body and the second for the myelin processes. Using a specific MBP cDNA probe, we have observed that MBP gene expression is not down-regulated in dysmyelinated animals (D. M. Pataky, H.S.K., and J.D.S., unpublished work). This suggests that the oligodendrocyte cell bodies survive the dysmyelination procedure and are a likely origin of subsequent myelin.

In conclusion, these findings demonstrate that suppression of myelination results in both neuroanatomical repair and functional CNS recovery after an embryonic spinal cord injury. Preliminary evidence also suggests that a slightly modified neuroimmunological approach will remove myelin from the post-hatchling spinal cord. It remains to be determined whether this intervention will improve the repair and recovery of function after injury to the adult spinal cord. Nevertheless, the present data clearly confirm and extend the proposition that the presence of CNS myelin contributes to the inhibition of neuronal repair after an adult CNS injury (3, 11, 12). This suggestion is also indirectly supported by the demonstration that lampreys, which do not have myelinated CNS axonal fiber tracts, are capable of functional regeneration after either a larval or an adult spinal cord injury (26).

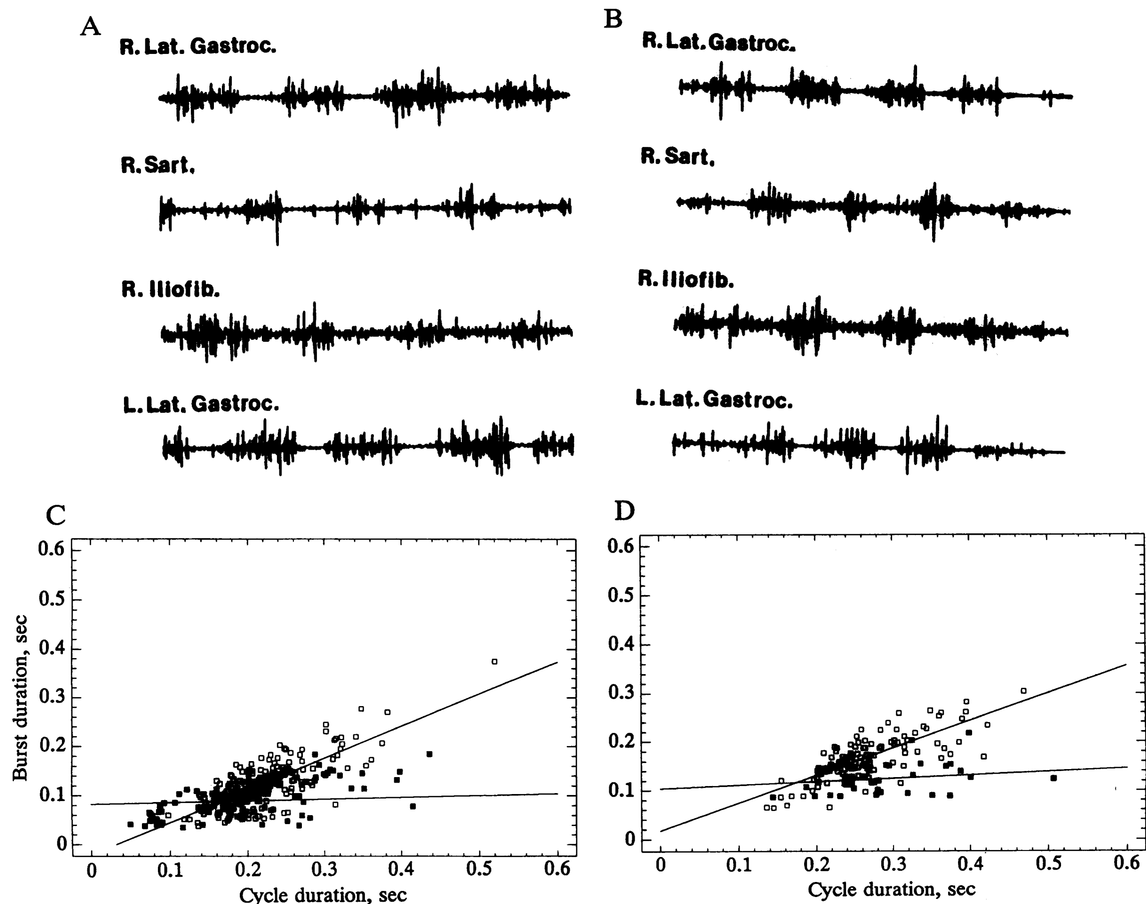

FIG. 3. (*A* and *B*) Simultaneous EMG recordings from four leg muscles during over-ground walking by a normally myelinated, unoperated (control) chick (*A*) and a dysmyelinated, E15-transected chick (*B*). The dysmyelinated E15-transected chick shows the same muscle activity patterns as the control chick. R., right; L., left; Lat., lateral; Gastroc., gastrocnemius; Sart., sartorius; Iliofib., iliofibularis. (*C*) Regression of muscle activity (burst) duration versus step cycle duration for lateral gastrocnemius muscle (□) and sartorius muscle (■) during over-ground walking by a normally myelinated, untransected hatchling chick. The burst duration of the lateral gastrocnemius muscle increases with increasing cycle duration, while the burst duration of the sartorius muscle remains constant as cycle duration increases. (*D*) Regression of burst duration versus step cycle duration for lateral gastrocnemius muscle (□) and sartorius muscle (■) during over-ground walking by a dysmyelinated, E15-transected hatchling chick. This animal displays the same relationships as the control animal in *C*. The slopes of corresponding regression lines in *C* and *D* are not significantly different. All regressions are significant to $P < 0.05$. The coefficients of determination (r^2) for lateral gastrocnemius and sartorius are 0.58 and 0.04 in *C* and 0.59 and 0.08 in *D*.

We thank Narinder Dhatt, Steve Katz, Doug Poirier, and Ania Wisniewska for technical assistance. We are indebted to Dr. Wilf Jeffries for counsel on immunological control experiments. This study was supported by grants (to J.D.S.) from the British Columbia Health Research Foundation and the Canadian Networks of Centers of Excellence (NCE) for Neural Regeneration and Functional Recovery. H.S.K. and S.J.H. were supported by predoctoral fellowships from NCE and the Natural Sciences and Engineering Research Council of Canada, respectively. G.D.M. was supported by a postdoctoral fellowship from the Medical Research Council of Canada.

1. Sholomenko, G. N. & Steeves, J. D. (1987) *Exp. Neurol.* **95**, 403–418.
2. Eidelberg, E. (1981) *Prog. Neurobiol.* **17**, 185–202.
3. Ramon y Cajal, S. (1913–1914) *Degeneration and Regeneration of the Nervous System*; trans. May, R. M., DeFelipe, J. & Jones, E. G. (1991), History of Neuroscience Series (Oxford Univ. Press, New York).
4. David, S. & Aguayo, A. J. (1981) *Science* **214**, 931–933.
5. Steeves, J. D., Sholomenko, G. N. & Webster, D. M. S. (1987) *Brain Res.* **401**, 205–212.
6. Glover, J. C. & Petursdottir, G. (1991) *J. Neurobiol.* **22**, 353–376.
7. Okado, N. & Oppenheim, R. W. (1985) *J. Comp. Neurol.* **232**, 143–161.
8. Shimizu, I., Oppenheim, R. W., O'Brien, M. & Schneiderman, A. (1990) *J. Neurobiol.* **21**, 918–937.
9. Hasan, S. J., Nelson, B. H., Valenzuela, J. I., Keirstead, H. S., Schull, S. E., Ethell, D. W. & Steeves, J. D. (1991) *Restor. Neurol. Neurosci.* **2**, 137–154.
10. Hasan, S. J., Keirstead, H. S., Muir, G. D. & Steeves, J. D. (1993) *J. Neurosci.*, in press.
11. Caroni, P. & Schwab, M. E. (1988) *Neuron* **1**, 85–96.
12. Schnell, L. & Schwab, M. E. (1990) *Nature (London)* **343**, 269–272.
13. Bensted, J. P. M., Dobbing, J., Morgan, R. S., Reid, R. T. W. & Payling Wright, G. (1957) *J. Embryol. Exp. Morphol.* **5**, 428–437.
14. Hartman, B. K., Agrawal, H. C., Kalmbach, S. & Shearer, W. T. (1979) *J. Comp. Neurol.* **188**, 273–290.
15. Macklin, W. B. & Weill, C. L. (1985) *Dev. Neurosci.* **7**, 170–178.
16. Hamburger, V. & Hamilton, H. L. (1951) *J. Morphol.* **165**, 49–92.
17. Hollyday, M. & Hamburger, V. (1977) *Brain Res.* **132**, 197–208.
18. Valenzuela, J. I., Hasan, S. J. & Steeves, J. D. (1990) *Dev. Brain Res.* **56**, 13–18.
19. Ranscht, B., Clapshaw, P. A., Price, J., Noble, M. & Seifert, W. (1982) *Proc. Natl. Acad. Sci. USA* **79**, 2709–2713.
20. Dorfman, S. H., Fry, J. M. & Silberberg, D. H. (1979) *Brain Res.* **177**, 105–114.
21. Dyer, C. A. & Benjamins, J. A. (1990) *J. Cell Biol.* **111**, 625–633.
22. Sergott, R. C., Brown, M. J., Silberberg, D. H. & Lisak, R. P. (1984) *J. Neurol. Sci.* **64**, 297–303.
23. Ozawa, K., Saida, T., Saida, K., Nishitani, H. & Kameyama, M. (1989) *Acta Neuropathol.* **77**, 621–628.
24. Mastaglia, F. L., Carroll, W. M. & Jennings, A. R. (1989) *Clin. Exp. Neurol.* **26**, 33–44.
25. Kosik, K. S. & Finch, E. A. (1987) *J. Neurosci.* **7**, 3142–3153.
26. McClellan, A. D. (1990) *Neuroscience* **37**, 781–798.